

Betelgeuse — Long Secondary Period, a Fundamental Mode and Overtones

Thomas Granzer,¹ Michael Weber,¹ Klaus G. Strassmeier,¹ and Andrea Dupree²

¹Leibniz Institute for Astrophysics Potsdam (AIP), Potsdam, Germany

²Harvard-Smithsonian Center for Astrophysics, Cambridge, MA, US

Abstract

Betelgeuse is the brightest Red Supergiant (RSG) in the sky and thus has been studied over decades. Photometrically, a fundamental pulsation mode (FM) at a period $P \approx 400$ d and a long, secondary period (LSP) with still disputed origin at $P \approx 2400$ d have been found. The Leibniz Institute for Astrophysics Potsdam (AIP) monitors Betelgeuse almost nightly since more than a decade with its robotic spectroscopic telescope STELLA, collecting $R \approx 55000$ spectra covering wavelength ranges from 390–860 nm. This proceeding reports about radial-velocity data, periods found within and their connection to photometric measurements.

1 Introduction

Betelgeuse (α Ori) is the closest red supergiant (RSG), spectral type M2Iab. It is commonly believed to be in core He burning phase. Its comparable proximity makes it also one of the biggest stars in the sky with an apparent diameter of $d \approx 0.042''$ in IR (Montargès *et al.*, 2014). This high apparent diameter hampers also the measurement of its parallax; its distance is estimated between 150–200 pc (Harper *et al.*, 2017). From this uncertainty in the distance, the determination of its luminosity, radius, and mass suffers, but it is generally accepted that Betelgeuse has a present-day mass of below $20 M_{\odot}$, a luminosity in the order of $10^5 L_{\odot}$, and a radius below $1000 R_{\odot}$. Refer to, e.g., Dolan *et al.* (2016).

Due to its high apparent diameter, direct imaging techniques can be used. Gilliland & Dupree (1996) were able to obtain the first direct image of a star except our Sun. Recent observations in Montargès *et al.* (2021) showed a dusty veil obscuring the SE-region of Betelgeuse during the great dimming event in Jan./Feb. 2020.

Early on, it was established that the radial velocity of Betelgeuse varies. A period close to $P \approx 5.8$ yrs has been reported already by Spencer Jones (1928), close to the long secondary period (LSP). Pulsation in the fundamental mode (FM) with a period close to $P \approx 400$ d has been published by Smith *et al.* (1989). Goldberg (1984) reports a lag in the RV observations with respect to the photometric variations. Kiss *et al.* (2006) use AAVSO photometric data¹ to derive a primary period of the FM of $P = 388 \pm 30$ d and a LSP of $P = 2050 \pm 460$ d. Later, Joyce *et al.* (2020) claim the discovery of the first overtone to the FM at a period of $P = 185.5$ d. Time-frequency analysis of the photometric data have been performed by Kolláth & Csubry (2006).

2 Observations

Radial velocities (RV) have been determined from spectra obtained with the STELLA robotic observatory (Strassmeier

et al., 2004) using the STELLA échelle spectrograph (SES). SES is a fiber-fed, white-pupil échelle spectrograph with a resolution of $R \approx 55000$. The wavelength range of $\lambda\lambda$ 390–870 nm is covered in a fixed format. The optical bench is thermally stabilized at an RMS scatter of 0.68°C , which allows for a long-term stability at an error down to $\approx 50\text{m/s}$ (Weber *et al.*, 2012). External errors are controlled via nightly observations of Coravel radial velocity standards (Udry *et al.*, 1999). The radial velocity is derived via cross-correlating the observed spectra to an appropriate template spectra on a per-order basis. The RV is the weighted average of the derived per-order shifts. Errors of the RV are from the standard deviation.

Observations started in Oct. 2008 and are still ongoing. To date, more than 4000 data points have been collected. During all these years, the spectrograph stayed almost identically, except for an exchange of the camera (2011), the cross-disperser (2012) and the introduction of a beam-splitter (2014). No systematic shifts in the RV data were experienced at these dates.

3 Results

The entire data set is depicted along with AAVSO Johnson-V photometry in Fig. 1. RV is plotted such that blue shift is up to emphasize the similarity with photometry. Both, a long period of order ≈ 2000 days and a shorter one resembling the fundamental mode are immediately visible. Fig 2 shows a zoom-in of the data starting a season prior to the great dimming event. Here the time lag of ≈ 30 d of the RV against the photometric signal is clearly seen.

A generalized Lomb-Scargle (GLS, Zechmeister & Kürster (2009)), shown in Fig. 3 of the entire RV data set shows the highest peak at an $f = 0.4535 \cdot 10^{-3} \text{cy/d}$ or at a period of $P = 2205$ d. Fitting a sine-wave to the RV data fixes the period at $P = 2169 \pm 5.3$ d, the peak-to-valley amplitude at $2A = 5.36 \pm 0.056$ km/sec, and the system velocity at $\gamma = 20.57 \pm 0.017$ km/sec, where the errors are formal errors derived from the covariance matrix of the final fit.

¹<https://www.aavso.org>

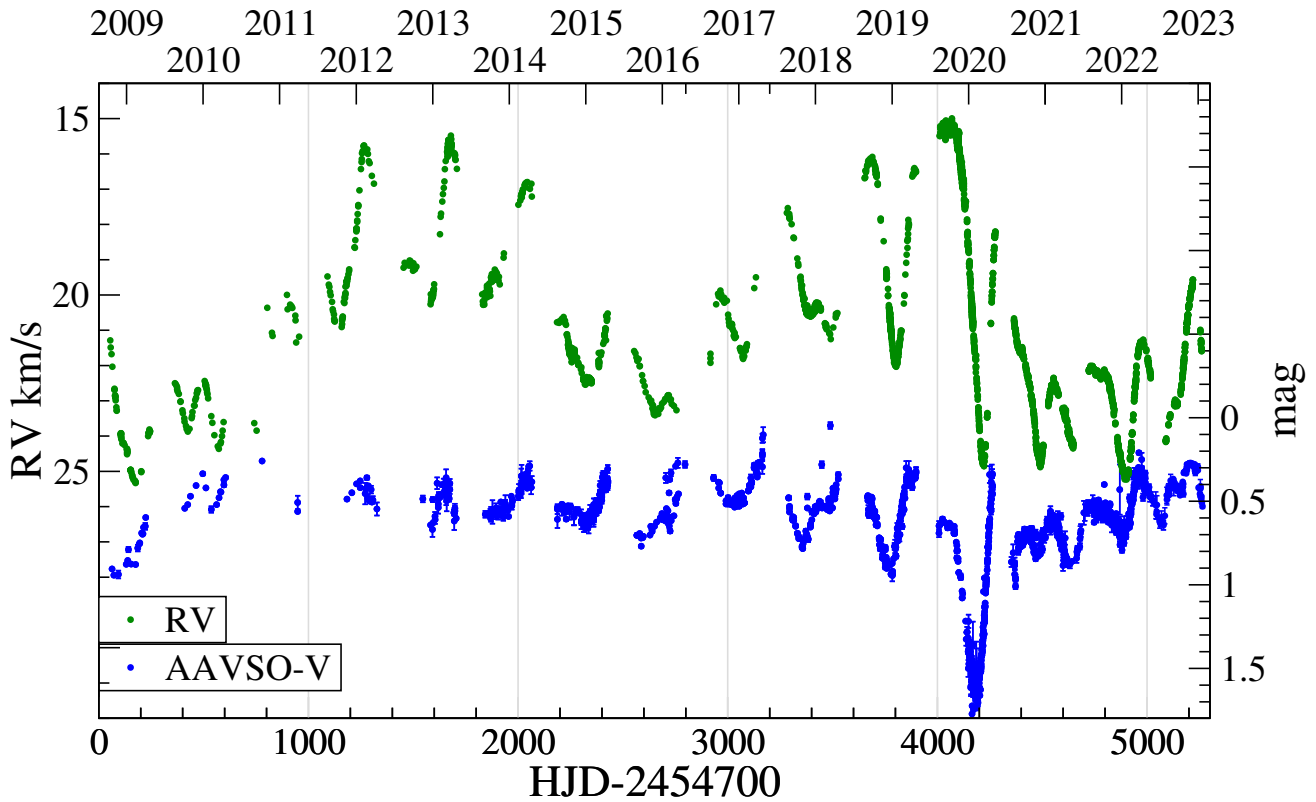


Figure 1: Radial velocity (RV) of Betelgeuse as derived via cross-correlation from high-resolution spectra shown in green. For comparison, AAVSO-photometry is plotted as blue dots spanning the same time range as the RV data. RV is plotted blue-shifted up to make the resemblance to photometry more easily seen.

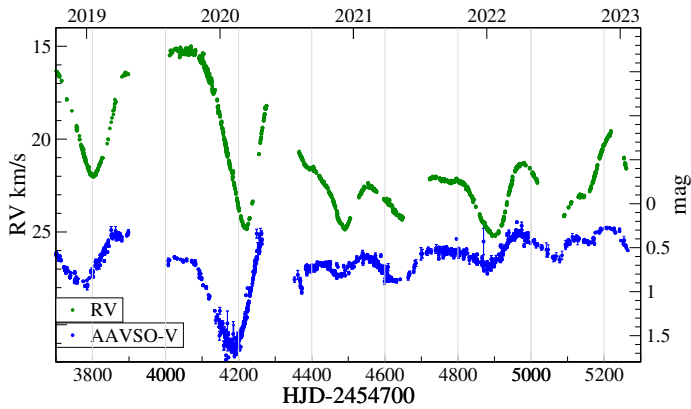


Figure 2: A zoom-in of Fig.1 starting with data one season prior to the great dimming event until now. The time-lag of the radial velocity data in the order of ≈ 30 d is easily seen. Note also the shorter periodicity in both, RV and photometric data, after the great dimming.

This period coincides well with the photometrically claimed LSP of Betelgeuse. Fig. 4 shows the data and the sinusoidal fit in green. The fit is not perfect, for comparison, a smoothing-spline interpolation of the data is overplotted in blue. Both, the green and the blue curve, show that the great dimming is far from an extremal value of the LS periodicity,

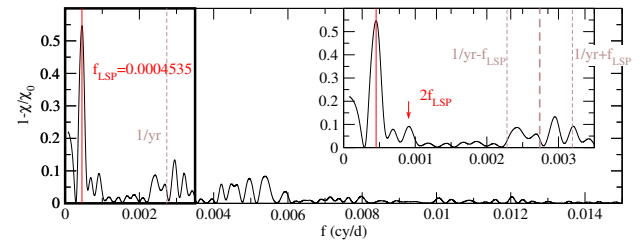


Figure 3: A generalized Lomb-Scargle periodogram of the RV data in Fig. 1. The long secondary period (LSP) sticks out as the by far highest peak. The insert shows the low- f range of the periodogram along with the $f_{\text{yr}} = 1/\text{yr}$ aliases as the dashed lines.

arguing against claims that an accidental coincidence of fundamental mode and LSP extremal values has caused the great dimming.

To clearly reveal the fundamental mode and to separate possible $f = 1/\text{yr} \pm f_{\text{LSP}}$ aliases from the data, we proceed in pre-whitening the LSP from the data. Two methods, removing a pure sinusoidal signal and the spline-smoothed interpolation agreed in the principal conclusions, but the signal is more clearly revealed in the spline-whitened data set. A GLS of this data is shown in Fig. 5. Here, the fundamental mode sticks out at $f^0 = 2.535 \cdot 10^{-3} \text{ cy/d}$, or at $P^0 = 394.5 \text{ d}$. The second-highest peak (ignoring the 1-year alias to f^0) is the

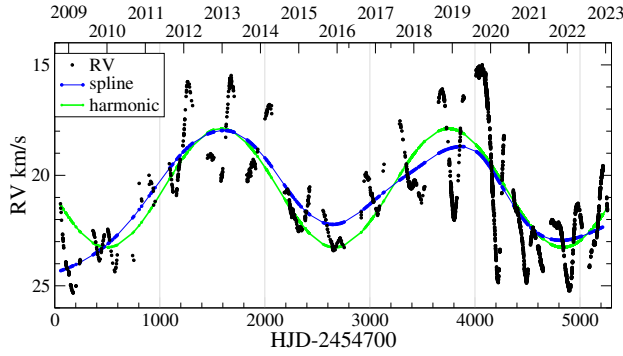


Figure 4: The RV data along with a pure sinusoidal fit to the LSP in green. For comparison, a smoothing-spline interpolation in blue is shown. Both fits suggest that the LSP-extremas do not coincide with the great dimming event.

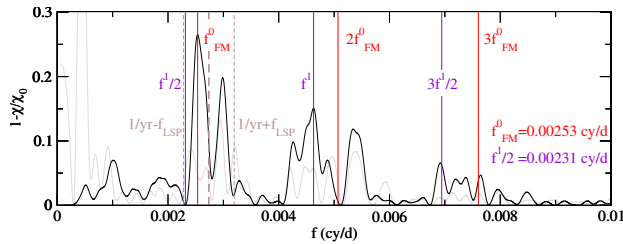


Figure 5: A generalized Lomb-Scargle periodogram of the RV data after removal of the LSP via the smoothing spline in Fig. 4. The fundamental mode f^0 is now the highest peak. Its alias to the 1/yr frequency is also clearly seen. The second highest peak is labeled f^1 and is identified with the first overtone (see text). Some evidence of the second overtone between $3/2 \cdot f^1$ and $3f^0$ can be seen.

first overtone at $f^1 = 4.629 \cdot 10^{-3}$ cy/d, or at $P^1 = 216.0$ d, which is at a slightly lower frequency (longer period) than twice the fundamental mode, but rather at a ratio of $f^1/f^0 \approx 1.83$. This is a rather surprising fact, though a similar deviation from a stringent 1:2 frequency ratio has been reported for semiregular and Mira variables (Kiss *et al.* (1999), Molnár *et al.* (2019)). The GLS also shows some evidence for the second overtone, in the range of $f^2 = 0.007 \dots 0.008$ cy/d, Fig 5.

The great dimming is believed to have been caused by a coronal mass ejection (CME) on Betelgeuse followed by a cooling of the ejected material and a partly blocking of Betelgeuse's light in the aftermath, (Dupree *et al.* (2022), Dupree *et al.* (2020)). From Fig. 2 it is apparent that the pulsation state of Betelgeuse changed to half the period, i.e., the first overtone after the great dimming event. To investigate this further, we performed a time-frequency analysis using wavelets following the prescription in Foster (1996). The result can be seen in Fig. 6. One not only sees a slight variation in the period length of the fundamental mode, it is also apparent that pulsation in this FM stopped well before the great dimming event (marked in cyan for the time of maximal redshift), and a pulsation in the first overtone developed. This again supports the picture of a CME which took some time to expand and cool to form an absorbing dust cloud. Right now, Betelgeuse pulsates in the first overtone of the fundamental mode, maybe similar to a music instrument in its transient response.

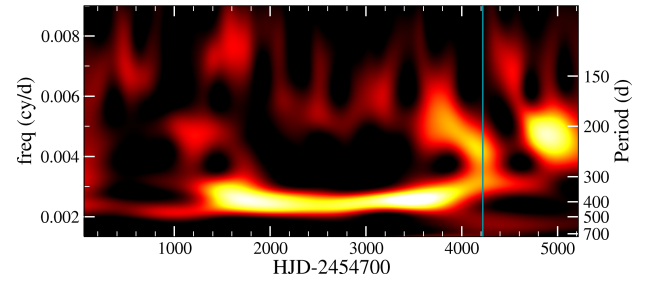


Figure 6: A wavelet analysis according to Foster (1996) of the entire RV data set. Note the switch-over to a pulsation in the first overtone well before the great dimming event (marked with a cyan line). Also note that the frequency of the fundamental mode is slightly varying and that the 1-year alias visible in Fig. 5 disappeared.

We will continue monitoring this interesting star.

References

- Dolan, M. M., Mathews, G. J., Lam, D. D., Quynh Lan, N., Herczeg, G. J., *et al.* 2016, *ApJ*, 819, 7.
 Dupree, A. K., Strassmeier, K. G., Calderwood, T., Granzer, T., Weber, M., *et al.* 2022, *ApJ*, 936, 18.
 Dupree, A. K., Strassmeier, K. G., Matthews, L. D., Uitenbroek, H., Calderwood, T., *et al.* 2020, *ApJ*, 899, 68.
 Foster, G. 1996, *AJ*, 112, 1709.
 Gilliland, R. L. & Dupree, A. K. 1996, *ApJL*, 463, L29.
 Goldberg, L. 1984, *PASP*, 96, 366.
 Harper, G. M., Brown, A., Guinan, E. F., O’Gorman, E., Richards, A. M. S., *et al.* 2017, *AJ*, 154, 11.
 Joyce, M., Leung, S.-C., Molnár, L., Ireland, M., Kobayashi, C., *et al.* 2020, *ApJ*, 902, 63.
 Kiss, L. L., Szabó, G. M., & Bedding, T. R. 2006, *MNRAS*, 372, 1721.
 Kiss, L. L., Szatmáry, K., Cadmus, J., R. R., & Mattei, J. A. 1999, *A&A*, 346, 542.
 Kolláth, Z. & Csabry, Z. 2006, *MmSAI*, 77, 109.
 Molnár, L., Joyce, M., & Kiss, L. L. 2019, *ApJ*, 879, 62.
 Montargès, M., Cannon, E., Lagadec, E., de Koter, A., Kervella, P., *et al.* 2021, *Nature*, 594, 365.
 Montargès, M., Kervella, P., Perrin, G., Ohnaka, K., Chavassa, A., *et al.* 2014, *A&A*, 572, A17.
 Smith, M. A., Patten, B. M., & Goldberg, L. 1989, *AJ*, 98, 2233.
 Spencer Jones, H. 1928, *MNRAS*, 88, 660.
 Strassmeier, K. G., Granzer, T., Weber, M., Woche, M., Andersen, M. I., *et al.* 2004, *Astronomische Nachrichten*, 325, 527.
 Udry, S., Mayor, M., Maurice, E., Andersen, J., Imbert, M., *et al.* 1999, In *IAU Colloq. 170: Precise Stellar Radial Velocities*, edited by J. B. Hearnshaw & C. D. Scarfe, *Astronomical Society of the Pacific Conference Series*, vol. 185, p. 383.
 Weber, M., Strassmeier, K. G., & Granzer, T. 2012, In *Astronomical Society of India Conference Series, Astronomical Society of India Conference Series*, vol. 7, p. 165.
 Zechmeister, M. & Kürster, M. 2009, *A&A*, 496, 577.